

Dynamic Characteristics of Multi-Disk Shaft System using the Vectors of Solution Coefficients

Z. Hamdi Cherif, Ch. Kandouci*

LSCMI Laboratory, Faculty of Mechanical Engineering,
University of Sciences and Technology USTO-MB of Oran,
Algeria

*ch.kandouci@gmail.com

ABSTRACT

In this paper, a technique using relationships between the coefficient vectors of the differential equation solutions is extended to calculate the five lowest forward and backward whirling speeds of a multi-disk shaft system. To this end, the vertical and horizontal components of transverse vibrations are analysed using the Bernoulli-Eulerbeam model, including the gyroscopic effect of each disk. The aforementioned relationships obtained from the continuity equation and the equilibrium equations, when written in matrix form and compared to the conventional transfer matrices related to the state vector, present an advantage that reduces the number of multiplied matrices, when adjacent shaft segments have the same material properties and/or diameters. The associated whirling mode shapes are determined using the algebraic complements according to I.P. Natanson. The good agreement via a comparison between the obtained results and those available in the literature shows the efficiency and the accuracy of the presented method.

Keywords: *shaft segment; vibration; constant coefficient vector; transfer matrix.*

Introduction

The increasing demand for rotating machinery subjected to wide range of speed changes requires an accurate determination of higher critical speeds. Many research papers have studied the dynamics of rotating machinery. In the first published work on the dynamics of rotating shafts presented by Rankine [1], the term whirling is introduced to mechanical engineering

practice. Dunkerley [2] published test results of rotor motion driven by belt transmission. He notices that under the slight unbalance its axis deviates from the bearing line to the point determined by a particular speed. After crossing it, the deviation amplitude decreases. According to Nelson [3], Dunkerley is the first who introduced the term "critical speed" to mechanical engineering. Green [4] considered the gyroscopic effect on critical speeds of flexible rotors using a lumped parameter system representation. Among other works devoted to whirling phenomenon, Eshleman and Eubanks [5] presented an analytical method for whirling speeds of a rotating shaft carrying "one" disk, Jun et al. [6] analysed the bending vibration of multi-stepped shaft using Timoshenko beam model including the gyroscopic effect due to a shaft rotation. Jong-Shyong Wu et al. [7] proposed an analytical solution for whirling speeds and mode shapes of a multi-disk shaft system, substituting the effect of each rigid disk by a lumped mass together with a frequency-dependent equivalent mass moment of inertia, and they compared the obtained numerical results using both analytical method and finite element method (FEM). In [7], the natural frequencies with their associated mode shapes and the whirling speeds are determined, however, the associated "whirling mode shapes" are not presented. In [5]-[7], the equations of vertical and horizontal vibrations of each shaft cross-section are combined to form one partial differential equation in a complex number and then the motion equation, the continuity equations, the equilibrium equations, and the associated boundary conditions are obtained in terms of the complex numbers.

Surovec et al. [8] investigated coupled torsional vibrations of rotating machine by means of Föppl-Jeffcott rotor to find a mathematical model, and to determine the natural frequency for both cases of damped and undamped free vibrations. Spagnol J. P. et al. [9] have applied Lagrangian mechanics and partial differential equations to develop an analytical model for the purpose of early fault-detection in rotor-bearing systems, with both symmetric and asymmetrical properties. Moradi Tiaki et al. [10] studied primary resonances of an overhung rotor taking into account rotary inertia and gyroscopic effects, using the multiple scales method to the discretized differential equations of motion. The transfer matrix method (TMM), for convenience, was introduced by Myklestad in 1944 and generalized by Prohl in 1945. In the field of rotor dynamics, the (TMM) has been widely applied both for eigen and response analysis. Lund et al. [11] extended the (TMM) for calculating the elliptical whirl orbits of a rotor, by including anisotropic characteristics of the fluid film bearings, which couple rotor motions in horizontal and vertical directions. Murphy et al. [12] developed a polynomial transfer matrix method to find all eigen values (critical speeds), which improved the (TMM) for eigen value calculations without missing any mode.

In the present paper, a shaft with symmetric properties in stiffness and inertia, carrying three rigid disks, and mounted on ball bearings used by

Jong-Shyong Wu et al. [7], is considered. The Bernoulli-Euler beam theory is used to describe the field properties of the shaft, in the case of a linear system including gyroscopic effect. The rotary inertia and transverse shear of the shaft are negligible when compared to the gyroscopic effects of the disks [5]. The transfer matrices related to the coefficient vectors of differential equation solutions are extended here to calculate natural frequencies and critical whirling speeds. The theory of this approach applied to forced vibrations of shafting system is proposed by Kolenda J. [13, 14]. In [15], this technique is used to analyse the forced axial and torsional vibrations of a real ship shaft line. This approach presents an advantage compared to the well-known (TMM) related to the state vector, it reduces the number of multiplied matrices, when adjacent shaft segments have the same material properties and/or diameters. The mode shapes corresponding to the natural frequencies and critical whirling speeds are computed using algebraic complements according to I.P. Natanson [16].

Physical Model of Multistep Shaft-Disk System

Physical model of shaft-disk system is shown in Figure 1. It concerns a multistep shaft carrying a rigid disk, with its two ends supported by ball bearing. The system is divided into series of n uniform shaft segments. The division is made at the section joining two shaft segments which have different constants of material or/and diameters, and at the section passing through the centre of gravity of discrete mass (disk i) joining two shaft segments (i) and ($i+1$)

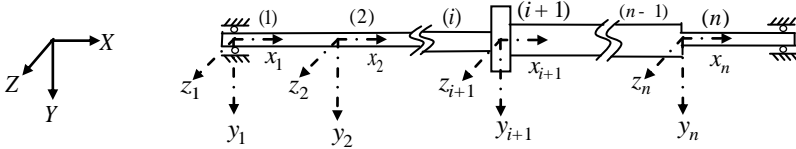


Figure 1: Physical model of the analyzed system.

It is assumed that the system is linear, and that each disk i represents a discrete mass. For each shaft segment (i), it is adopted a fixed coordinate system (x_i, y_i, z_i) whose axes are respectively parallel to the axes of the fixed reference system (X, Y, Z) . If the gyroscopic effect in the shaft is not considered, the differential equations governing transverse vibrations of the i th shaft segment are uncoupled and given by:

$$\rho_i S_i \frac{\partial^2 u_{y,i}(x,t)}{\partial t^2} + E_i I_i \frac{\partial^4 u_{y,i}(x,t)}{\partial x^4} = 0 \quad (1a)$$

$$\rho_i S_i \frac{\partial^2 u_{z,i}(x,t)}{\partial t^2} + E_i I_i \frac{\partial^4 u_{z,i}(x,t)}{\partial x^4} = 0 \quad (1b)$$

where E_i is the modulus of elasticity (N/m^2), S_i the cross-sectional area (m^2), I_i the diametric moment of inertia (m^4) of the i th shaft segment, and ρ_i is the density of the shaft material (kg/m^3), while $u_{y,i}$ is the vibration for the centroid of the cross-section of the i th shaft segment in the vertical direction (y), at axial coordinate $x = x_i$ and time t , $u_{z,i}$ denotes the transverse vibration in horizontal direction (z). For free vibrations:

$$u_{y,i}(x,t) = \bar{u}_{y,i}(x) e^{\pm j\tilde{\omega}t} \quad (2a)$$

$$u_{z,i}(x,t) = \bar{u}_{z,i}(x) e^{\pm j\tilde{\omega}t} \quad (2b)$$

with $j = \sqrt{-1}$, while, $\bar{u}_{y,i}(x)$ and $\bar{u}_{z,i}(x)$ are the shape functions of the vibrations and $\tilde{\omega}$ is the natural frequency of the shaft-disk system. The upper sign (+) and lower sign (-) are for the forward and backward whirls, respectively. Substituting Equations (2a) and (2b) into Equation (1a) and (1b):

$$\bar{u}_{y,i}(x) = a_{i1} \cos \lambda x + a_{i2} \sin \lambda x + a_{i3} \cosh \lambda x + a_{i4} \sinh \lambda x \quad (3a)$$

$$\bar{u}_{z,i}(x) = a_{i5} \cos \lambda x + a_{i6} \sin \lambda x + a_{i7} \cosh \lambda x + a_{i8} \sinh \lambda x \quad (3b)$$

with, $\lambda = \lambda_i = \omega^{1/2} (\rho_i S_i / E_i I_i)^{1/4}$.

The slopes are:

$$\theta_{z,i}(x,t) = \frac{\partial u_{y,i}(x,t)}{\partial x}, \quad \theta_{y,i}(x,t) = -\frac{\partial u_{z,i}(x,t)}{\partial x} \quad (4)$$

If designate $u_i = \{u_{y,i}, u_{z,i}, \theta_{y,i}, \theta_{z,i}\}$ as the vibration vector, will have:

$$u_i = \bar{u}_i(x) e^{\pm j\tilde{\omega}t} \quad (5)$$

Real part of this vector can be written in the form:

$$\bar{u}_i(x) = C_i(x) a_i \quad (6)$$

while, $a_i = \{a_{i1}, a_{i2}, \dots, a_{i8}\}$ is the vector of solution coefficients for the i th shaft segment. Internal forces and moments are:

$$T_{y,i}(x,t) = -EI_i \frac{\partial^3 u_{y,i}}{\partial x^3}, \quad T_{z,i}(x,t) = -EI_i \frac{\partial^3 u_{z,i}}{\partial x^3} \quad (7a)$$

$$M_{z,i}(x,t) = -EI_i \frac{\partial^2 u_{y,i}}{\partial x^2}, \quad M_{y,i}(x,t) = EI_i \frac{\partial^2 u_{z,i}}{\partial x^2} \quad (7b)$$

$T_{y,i}(x,t)$ and $T_{z,i}(x,t)$ are the shear forces in the y and z directions, respectively. The subscripts i and x refer to the i th shaft segment and its section, respectively. $M_{z,i}$ and $M_{y,i}$ are the bending moments in the vertical and horizontal planes. Taking into account Equation (5), these internal forces and moments can be expressed as:

$$T_{y,i}(x,t) = \bar{T}_{y,i}(x) e^{\pm j\tilde{\omega}t}, \quad T_{z,i}(x,t) = \bar{T}_{z,i}(x) e^{\pm j\tilde{\omega}t} \quad (8a)$$

$$M_{y,i}(x,t) = \bar{M}_{y,i}(x) e^{\pm j\tilde{\omega}t}, \quad M_{z,i}(x,t) = \bar{M}_{z,i}(x) e^{\pm j\tilde{\omega}t} \quad (8b)$$

$p_i = \{T_{y,i}, T_{z,i}, M_{y,i}, M_{z,i}\}$ is the vector of internal forces and moments:

$$p_i = \bar{p}_i(x) e^{\pm j\tilde{\omega}t} \quad (9)$$

$$\bar{p}_i(x) = D_i(x) a_i \quad (10)$$

The matrices $C_i(x)$ and $D_i(x)$ are written in the appendix. With the assumption that the shaft is simply supported in bearings at both ends, the boundary conditions are:

$$\bar{u}_{y,1}(0) = 0, \quad \bar{u}_{z,1}(0) = 0, \quad E_1 I_1 \bar{u}_{y,1}''(0) = 0, \quad E_1 I_1 \bar{u}_{z,1}''(0) = 0 \quad (11a)$$

$$\bar{u}_{y,n}(L) = 0, \quad \bar{u}_{z,n}(L) = 0, \quad E_n I_n \bar{u}_{y,n}''(L) = 0, \quad E_n I_n \bar{u}_{z,n}''(L) = 0 \quad (11b)$$

Transfer Matrices Related to Solution Coefficients

The case of shaft segments with different diameters (and/ or) different material properties

A model of two adjacent shaft segments is illustrated in Figure 2. $L_i = L$ denotes the length of the i th shaft segment:

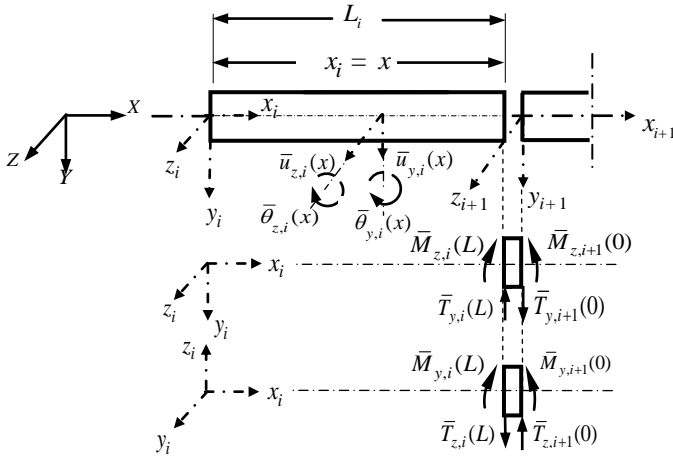


Figure 2: Schematic illustration of displacements and internal forces (moments) acting at the junction of two adjacent shaft segments (i) and ($i+1$).

At the junction of two shaft segments having different constants of material or/and diameters, the continuity equations for the deformations, and the equilibrium equations are:

$$\bar{u}_i(L) = \bar{u}_{i+1}(0) \quad (12)$$

$$\bar{p}_i(L) = \bar{p}_{i+1}(0) \quad (13)$$

Taking into account Equation (6) and (10), Equation (12) and Equation (13) can be written as:

$$C_i(L) a_i = C_{i+1}(0) a_{i+1} \quad (14)$$

$$D_i(L) a_i = D_{i+1}(0) a_{i+1} \quad (15)$$

$$B_i = \begin{bmatrix} C_{i+1,0} \\ D_{i+1,0} \end{bmatrix}^{-1} \begin{bmatrix} C_{i,L} \\ D_{i,L} \end{bmatrix} \quad (16)$$

The matrix B_i can be considered as a transfer matrix related to the solution coefficients, which has a block diagonal form (see appendix). For the $(s - 1)$ following shaft segments, the following relationship is derived:

$$a_{i+s} = B_{+s-1} B_{i+s-2} \dots B_i a_i. \quad (17)$$

In these calculations, the number of multiplied matrices in Equation (17) may be large, however, the matrices B_i have an advantageous convenience, when the shaft segments have the same material constants and diameters, and the Equation (17) is reduced to:

$$a_{i+s} = G_i a_i, \quad (18)$$

where the matrix G_i is obtained from the matrix B_i by setting:

$$(e_1)_i = (e_3)_i = 1, \quad (e_2)_i = (e_4)_i = 0$$

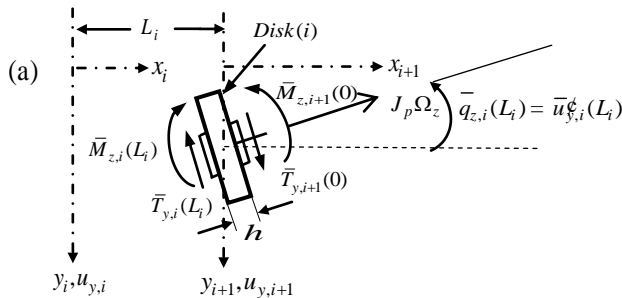
and replacing L_i by:

$$L_i = \sum_{p=i}^{p=i+s-1} L_p \quad (19)$$

(i.e. the multiplication of this type of transfer matrices in the case listed below, can be replaced by a summation of function arguments occurring in these matrices). This convenient property of presented approach does not exist with the well-known transfer matrices related to the state vector. An adoption of a linear model of internal damping in shafts does not eliminate the property of the presented method.

A case of a discrete mass (disk i) joining two shaft segments (i) and ($i+1$)

A case of simultaneous movements of whirling and spinning of a disc is shown in Figure A1 in the appendix. Figure 3(a) and Figure 3(b) show a case where two adjacent shaft segments (i) and ($i+1$) rotating with spin speed Ω and joined by a discrete mass m_i (disk (i)), with inertia matrix M_i , on the vertical and horizontal planes, respectively.



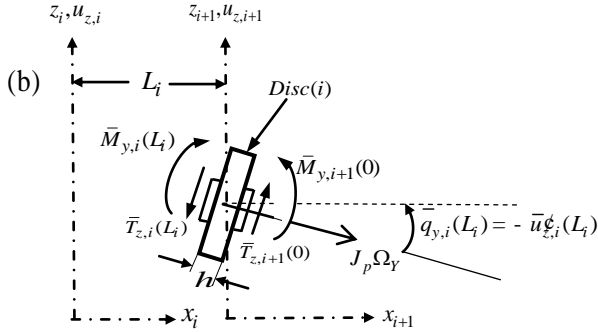


Figure 3: Forces and moments acting on rigid disk i joining two shaft segments (i) and ($i+1$) on (a) the xy -plane, and (b) the xz -plane.

The components of the angular speed Ω are:

$$\Omega_y = \Omega \sin \theta_{z,i}(L_i, t) \approx \Omega \theta_{z,i}(L_i, t) \quad (20a)$$

$$\Omega_z = \Omega \sin(-\theta_{y,i}(L_i, t)) \approx -\Omega \theta_{y,i}(L_i, t) \quad (20b)$$

Under the assumption that the displacements are small and the centre of gravity of the disk i is coincident with the centroid of the cross-section of the shaft segment, the following conditions are verified:

$$\bar{u}_i(L) = \bar{u}_{i+1}(0) \quad (21)$$

$$T_{y,i}(L, t) = T_{y,i+1}(0, t) - m_i \frac{\partial^2 u_{y,i}(L, t)}{\partial t^2} \quad (22a)$$

$$T_{z,i}(L, t) = T_{z,i+1}(0, t) - m_i \frac{\partial^2 u_{z,i}(L, t)}{\partial t^2} \quad (22b)$$

$$M_{y,i}(L, t) = M_{y,i+1}(0, t) - J_{d,i} \frac{\partial^2 \theta_{y,i}(L, t)}{\partial t^2} - J_{p,i} \frac{\partial \Omega_y}{\partial t} \quad (23a)$$

$$M_{z,i}(L, t) = M_{z,i+1}(0, t) - J_{d,i} \frac{\partial^2 \theta_{z,i}(L, t)}{\partial t^2} - J_{p,i} \frac{\partial \Omega_z}{\partial t} \quad (23b)$$

where $J_{d,i}$ and $J_{p,i}$ are the diametric and polar mass moments of inertia of the disk i , respectively. The gyroscopic moments of the disk i couple the equilibrium equations for the moments (23a) and (23b). Substituting Equation (20a) and (20b) into Equation (23a) and (23b), respectively, and get:

$$\bar{M}_{y,i}(L) - J_{d,i} \tilde{\omega}^2 \bar{\theta}_{y,i}(L) + jJ_{p,i} \Omega \tilde{\omega} \bar{\theta}_{z,i}(L) = \bar{M}_{y,i+1}(0) \quad (24a)$$

$$\bar{M}_{z,i}(L) - J_{d,i} \tilde{\omega}^2 \bar{\theta}_{z,i}(L) - jJ_{p,i} \Omega \tilde{\omega} \bar{\theta}_{y,i}(L) = \bar{M}_{z,i+1}(0) \quad (24b)$$

Introducing Equation (7a) and (7b) into Equation (22a), (22b), (24a) and (24b), and taking into account Equation (6), (8a) and (8b), the continuity equations for the vibrations and the equilibrium equations for the forces (and moments) can be written as:

$$C_i(L) a_i = C_{i+1}(0) a_{i+1} \quad (25a)$$

$$-(EI_z)_i \bar{u}_{y,i}''(L) - \tilde{\omega}^2 m_i \bar{u}_{y,i}(L) = -(EI_z)_{i+1} \bar{u}_{y,i+1}''(0) \quad (25b)$$

$$-(EI_y)_i \bar{u}_{z,i}''(L) - \tilde{\omega}^2 m_i \bar{u}_{z,i}(L) = -(EI_y)_{i+1} \bar{u}_{z,i+1}''(0) \quad (25c)$$

$$(EI_y)_i \bar{u}_{z,i}''(L) - J_{d,i} \tilde{\omega}^2 \bar{\theta}_{y,i}(L) + jJ_{p,i} \Omega \tilde{\omega} \bar{\theta}_{z,i}(L) = (EI_y)_{i+1} \bar{u}_{z,i+1}''(0) \quad (25d)$$

$$-(EI_z)_i \bar{u}_{y,i}''(L) - J_{d,i} \tilde{\omega}^2 \bar{\theta}_{z,i}(L) - jJ_{p,i} \Omega \tilde{\omega} \bar{\theta}_{y,i}(L) = -(EI_z)_{i+1} \bar{u}_{y,i+1}''(0) \quad (25e)$$

Equation (25b), (25c), (25d) and (25e) can be written in the following matrix form:

$$D_i(L) a_i - \tilde{\omega}^2 M_i C_i(L) a_i + jJ_{p,i} \Omega \tilde{\omega} S_i(L) a_i = D_{i+1}(0) a_{i+1} \quad (26)$$

The matrices $S_i(L)$ and M_i are given in the appendix, while:

$$a_i = [a_{i1}, a_{i2}, \dots, a_{i8}]^T. \quad (27)$$

According to Equation (25a), (26) and (27):

$$a_{i+1} = H_i a_i \quad (28)$$

where,

$$H_i = \begin{bmatrix} C_{i+1}(0) \\ D_{i+1}(0) \end{bmatrix}^{-1} \begin{bmatrix} C_i(L) \\ D_i(L) - \omega^2 M_i C_i(L) + j \Omega \omega J_{p,i} S_i(L) \end{bmatrix} \quad (29)$$

H_i is a transfer matrix related to the vector of solution coefficients a_i , through the disk i , taking into account its gyroscopic effect. Using the above derived transfer matrices, it can determine the vectors of solution coefficients a_2, a_3, \dots, a_n for the vibrations from the second to the n th shaft segments, as function of a_1 , which is the solution coefficient vector for vibrations of the first shaft segment. As an example, for the system illustrated in Figure 2, the following relationships are obtained:

$$\begin{aligned}
 a_2 &= B_1 a_1, \\
 a_3 &= B_2 a_2 = B_2 B_1 a_1 \\
 a_4 &= H_3 a_3 = H_3 B_2 B_1 a_1 \\
 &\vdots \\
 a_n &= B_{n-1} \dots H_3 B_2 B_1 a_1.
 \end{aligned} \tag{30}$$

The boundary conditions at the left and right pinned ends

Finally, the boundary conditions (11a) and (11b) can be written respectively as:

$$Q_1(0) a_1 = 0 \tag{31a}$$

$$Q_n(L_n) a_n = 0 \tag{31b}$$

The matrices $Q_1(0)$ and $Q_n(L_n)$ are written in the appendix. Substituting the relationships (30) into Equation (31a) and (31b), the resulting expressions can be written in the following matrix form:

$$\begin{bmatrix} Q_1(0) \\ Q_n(L_n) B_{n-1} \dots H_3 B_2 B_1 \end{bmatrix} \{a_1\} = 0 \tag{32}$$

thus, the boundary conditions (11a) and (11b) are expressed as a function of $\{a_1\}$, which is the constant coefficient column vector (8 x 1) of free vertical and horizontal vibrations of the first shaft segment ($i=1$):

$$\{a_1\} = [a_{11}, a_{12}, a_{13}, a_{14}, a_{15}, a_{16}, a_{17}, a_{18}]^T \tag{33}$$

According to Equation (32), the vector of constant coefficients $\{a_1\}$ verify the following equation:

$$D_1 \{a_1\} = 0 \tag{34}$$

where,

$$D_1 = \begin{bmatrix} d_{11} & d_{12} & \dots & d_{18} \\ d_{21} & \dots & & \\ \vdots & & & \\ d_{81} & \dots & & d_{88} \end{bmatrix} = \begin{bmatrix} Q_1(0) \\ Q_n(L_n) B_{n-1} \dots H_3 B_2 B_1 \end{bmatrix} \tag{35}$$

Equation (34) represents the characteristic equation for the vibrating system. Non-trivial solution for the vector of constant coefficients $\{a_1\}$, requires that:

$$|D_1| = 0 \tag{36}$$

which is the frequency equation. Natural frequencies (ω_r) of the non-rotating system and critical whirling speeds ($\tilde{\omega}_r$) may be obtained by solving the eigenvalue Equation (36), for ($\Omega = 0$) and ($\Omega = \omega_r$), respectively. For that, a technique used here, is that if the “product” for the values of the coefficient determinants $\Delta(\omega_k)$ and $\Delta(\omega_{k+1})$ is less than or equal to zero (i.e., $\Delta(\omega_k) \times \Delta(\omega_{k+1}) \leq 0$) with $\omega_{k+1} = \omega_k + \Delta\omega$, then the corresponding natural frequency ω_r is determined by the obtained value $\omega_k + 0.5\Delta\omega$. In the case of critical speed $\tilde{\omega}_r$, the matrix D_1 is complex and a similar technique is used.

Because the matrix D_1 is singular, the vector $\{a_1\}$ in Equation (34) can be estimated up to a multiplicative constant ϕ [16]:

$$a_{11} = \phi g_{11}, \quad a_{12} = \phi g_{12}, \quad a_{13} = \phi g_{13}, \dots, \quad a_{18} = \phi g_{18} \tag{37}$$

where $g_{1\alpha}$ ($\alpha = 1, \dots, 8$) are the algebraic complements of corresponding elements $d_{1\alpha}$ ($\alpha = 1, \dots, 8$) of the matrix D_1 .

$$g_{11} = \begin{vmatrix} d_{22} & d_{23} & \dots & d_{28} \\ d_{32} & \dots & & \\ \vdots & & & \\ d_{82} & \dots & & d_{88} \end{vmatrix}, \dots, \quad g_{18} = \begin{vmatrix} d_{21} & d_{22} & \dots & d_{27} \\ d_{31} & \dots & & \\ \vdots & & & \\ d_{81} & \dots & & d_{87} \end{vmatrix} \tag{38}$$

Thus,

$$\bar{u}_{y,1}(x) = g_{11} \cos \lambda_1 x + g_{12} \sin \lambda_1 x + g_{13} \cosh \lambda_1 x + g_{14} \sinh \lambda_1 x \tag{39}$$

$$\bar{u}_{z,1}(x) = g_{15} \cos \lambda_1 x + g_{16} \sin \lambda_1 x + g_{17} \cosh \lambda_1 x + g_{18} \sinh \lambda_1 x \tag{40}$$

with,

$$g_1 = \{g_{11}, g_{12}, \dots, g_{18}\}.$$

The functions (39) and (40) represent the mode shapes of vertical and horizontal vibrations, respectively, of the first shaft segment. The resultant of these functions represents the transverse mode shape. For the second shaft segment:

$$\bar{u}_2(x) = \begin{Bmatrix} \bar{u}_{y,2}(x) \\ \bar{u}_{z,2}(x) \end{Bmatrix} = C_2(x) \mathbf{g}_2 \tag{41}$$

with,

$$g_2 = \{g_{21}, g_{22}, \dots, g_{28}\}.$$

Based on Equation (30), the relationships for the rest of shaft segments are:

$$\begin{aligned} g_2 &= B_1 g_1, \\ g_3 &= B_2 g_2 = B_2 B_1 g_1 \\ g_4 &= H_3 g_3 = H_3 B_2 B_1 g_1 \\ &\dots \end{aligned} \tag{42}$$

$$g_n = H_{n-1} g_{n-1} = H_{n-1} H_{n-2} \dots H_3 B_2 B_1 g_1$$

where,

$$g_i = \{g_{i1}, g_{i2}, \dots, g_{i8}\}.$$

Description of the Analysed System

A shaft carrying three identical rigid disks as shown in Figure 4 is studied.

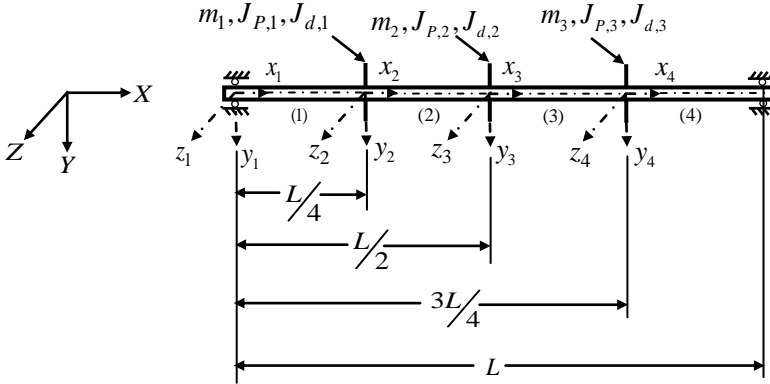


Figure 4: Analysed multi-disk shaft system.

Each disk with thickness of $h = 0.004 \text{ m}$, diameter of $d_d = 0.36 \text{ m}$ connected by four distributed shaft elements each with length of $L_t = 0.30 \text{ m}$ and diameter $d_s = 0.02 \text{ m}$, Young's modulus $E = 2.068 \cdot 10^{11} \text{ N/m}^2$, and the mass density for the disk (or shaft) material is $\rho_d = \rho_s = 7850 \text{ kg/m}^3$. This example is considered in [7], where the lowest five natural frequencies, natural mode shapes and whirling speeds are calculated.

The eigen value Equation (36) is solved using a developed program with the assistance of MATLAB. It is to be noted that the vibration Equations (1a) and (1b) do not contain any term likely to limit the amplitudes of free vibrations. For that, the obtained mode shapes using the algebraic complements according to I. P. Natanson [16] are normalized such that the maximum value of each mode is equal to unity. Table 1 shows the lowest five natural frequencies obtained from the presented method for the non-rotating system ($\Omega = 0$). The associated natural mode shapes of vertical and horizontal vibrations, shown in Figures (5-9) are the same since governed by the similar differential Equations (1a) and (1b), due to the assumption that the shaft has symmetric properties in stiffness and inertia. The resultant natural transverse mode shapes are plotted in Figures 10-14.

Table 1: The lowest five natural frequencies $\omega_1 - \omega_5$ (with $\Omega = 0$) for the analysed system (see Figure 4) obtained from the presented method and those obtained using FEM in [7]

Mode	Natural frequencies ω_r (rad / s) (with $\Omega = 0$)	
	Presented study	FEM in ref. [7]
1 st	75.39731	75.3973
2 nd	290.86410	290.8641
3 rd	611.95860	611.9586
4 th	958.47733	958.4773
5 th	1288.89180	1288.8920

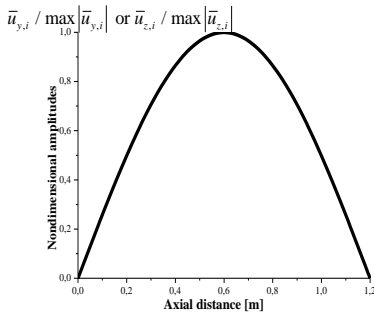


Figure 5: The first natural mode shape of vertical or horizontal flexural vibrations.

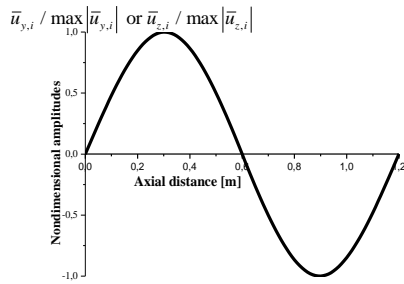


Figure 6: The second natural mode shape of vertical or horizontal flexural vibrations.

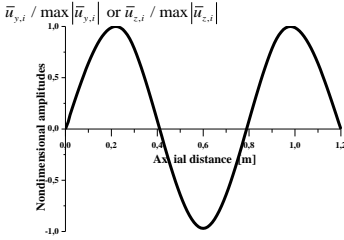


Figure 7: The third natural mode shape of vertical or horizontal flexural vibrations.

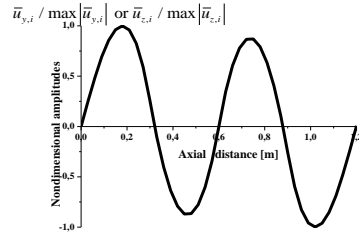


Figure 8: The fourth natural mode shape of vertical or horizontal flexural vibrations.

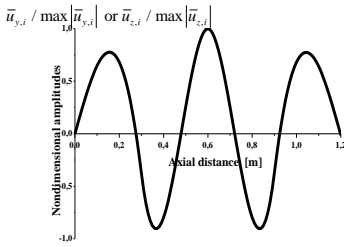


Figure 9: The fifth natural mode shape of vertical or horizontal flexural vibrations.

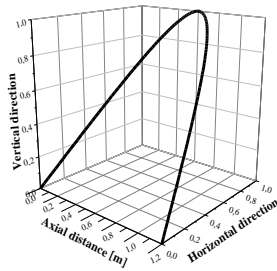


Figure 10: The first natural mode shape of transverse vibrations.

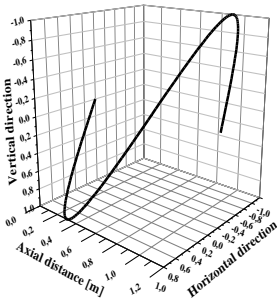


Figure 11: The second natural mode shape of transverse vibrations.

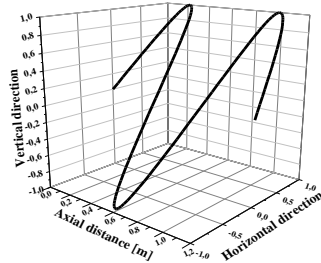


Figure 12: The third natural mode shape of transverse vibrations.

Table 2: The lowest five whirling speeds $\tilde{\omega}_1 - \tilde{\omega}_5$ (with $\Omega = \tilde{\omega}$) for the analysed system (see Figure 4) obtained from the presented method and those obtained using FEM in [7].

Direction of whirling	Whirling speeds $\tilde{\omega}_r$ (rad / s) with $\Omega = \tilde{\omega}$		
	Presented study	FEM in ref. [7]	
Forward	$\tilde{\omega}_1^F$	77.10999	77.1099
	$\tilde{\omega}_2^F$	316.25910	316.2592
	$\tilde{\omega}_3^F$	686.80099	686.8000
	$\tilde{\omega}_4^F$	4406.50311	4406.5176
	$\tilde{\omega}_5^F$	4412.74362	4412.7581
Backward	$\tilde{\omega}_1^B$	73.5999	73.7625
	$\tilde{\omega}_2^B$	266.58580	266.5857
	$\tilde{\omega}_3^B$	513.78038	513.7804
	$\tilde{\omega}_4^B$	587.40753	587.407
	$\tilde{\omega}_5^B$	927.963559	927.6585

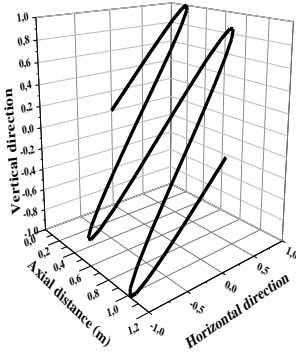


Figure 13: The fourth natural mode shape of transverse vibrations.

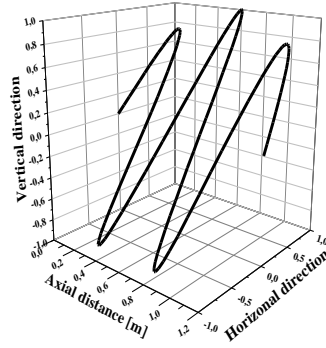


Figure 14: The fifth natural mode shape of transverse vibrations.

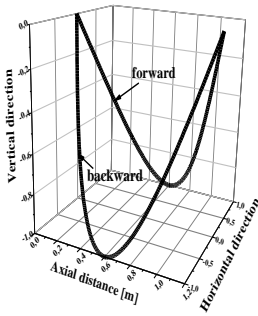


Figure 15: The first whirling mode shape.

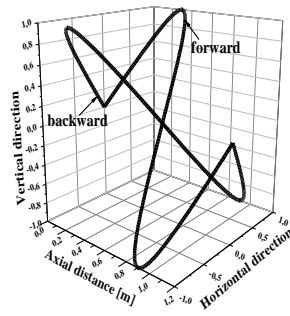


Figure 16: The second whirling mode shape.

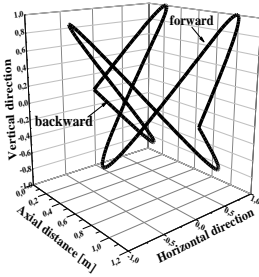


Figure 17: The third whirling mode shape.

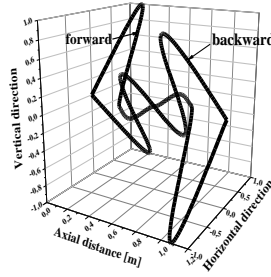


Figure 18: The fourth whirling mode shape.

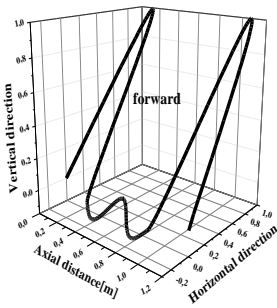


Figure 19: The fifth mode shape of forward whirl.

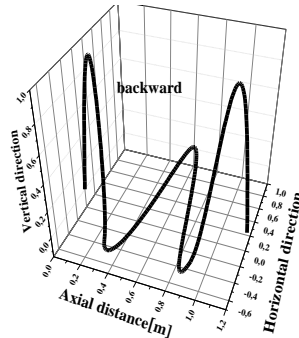


Figure 20: The fifth mode shape of backward whirl.

Conclusions

It is seen that the calculated natural frequencies as well as the critical whirling speeds agree perfectly with those obtained from existing literature ([7]). The given relationships in this work allow an analysis of the gyroscopic effect of disks on transverse vibrations. Especially, the extended transfer matrices related to the vectors of solution coefficients used in this work, are well-suited for manipulation and make the procedures straight forward for taking into account a linear model of internal damping in shafts or the consideration of shear effect, rotary inertia and transverse crack. The presented analytical method combined with algebraic complements, allows obtaining the natural mode shapes of multi-disk shaft system with appreciable accuracy. The presented technique is easy to compute and because of its reliability and precision, it can be used for vibration analysis of industrial rotating machinery, when the angular speed is subjected to wide ranges of change

APPENDIX

The matrices $C_i(x)$ and $D_i(x)$ in Equation (6) and (10) are as follows:

$$C_i(x) = \begin{bmatrix} \cos \lambda x & \sin \lambda x & \cosh \lambda x & \sinh \lambda x & 0 & 0 & 0 & 0 \\ 0 & 0 & 0 & 0 & \cos \lambda x & \sin \lambda x & \cosh \lambda x & \sinh \lambda x \\ 0 & 0 & 0 & 0 & \lambda \sin \lambda x - \lambda \cos \lambda x - \lambda \sinh \lambda x - \lambda \cosh \lambda x & & & \\ -\lambda \sin \lambda x \lambda \cos \lambda x \lambda \sinh \lambda x \lambda \cosh \lambda x & 0 & 0 & 0 & 0 & & & \end{bmatrix}$$

$$D_i(x) = E_i I_i \begin{bmatrix} -\lambda^3 \sin \lambda x \lambda^3 \cos \lambda x - \lambda^3 \sinh \lambda x - \lambda^3 \cosh \lambda x & 0 & 0 & 0 & 0 \\ 0 & 0 & 0 & 0 & -\lambda^3 \sin \lambda x \lambda^3 \cos \lambda x - \lambda^3 \sinh \lambda x - \lambda^3 \cosh \lambda x \\ 0 & 0 & 0 & 0 & -\lambda^2 \cos \lambda x - \lambda^2 \sin \lambda x \lambda^2 \cosh \lambda x \lambda^2 \sinh \lambda x \\ \lambda^2 \cos \lambda x \lambda^2 \sin \lambda x - \lambda^2 \cosh \lambda x - \lambda^2 \sinh \lambda x & 0 & 0 & 0 & 0 \end{bmatrix}$$

with $\lambda = \lambda_i = \tilde{\omega}^{1/2} (\rho_i S_i / E_i I_i)^{1/4}$, $x = x_i$; $0 \leq x_i \leq L_i$.

The matrix B_i in Eq. (16) has the following form:

$$B_i = \begin{bmatrix} B_i^{(1)} & 0 \\ 0 & B_i^{(2)} \end{bmatrix}, B_i^{(1)} = B_i^{(2)} = \begin{bmatrix} e_1 \cos \lambda L & e_1 \sin \lambda L & e_2 \cosh \lambda L & e_2 \sinh \lambda L \\ -e_3 \sin \lambda L & e_3 \cos \lambda L & e_4 \sinh \lambda L & e_4 \cosh \lambda L \\ e_2 \cos \lambda L & e_2 \sin \lambda L & e_1 \cosh \lambda L & e_1 \sinh \lambda L \\ -e_4 \sin \lambda L & e_4 \cos \lambda L & e_3 \sinh \lambda L & e_3 \cosh \lambda L \end{bmatrix}_{(i)}$$

where,

$$(e_1)_i = \frac{1}{2} + \frac{(EI\lambda^2)_i}{2(EI\lambda^2)_{i+1}}, \quad (e_2)_i = \frac{1}{2} - \frac{(EI\lambda^2)_i}{2(EI\lambda^2)_{i+1}},$$

$$(e_3)_i = \frac{\lambda_i}{2\lambda_{i+1}} + \frac{(EI\lambda^3)_i}{2(EI\lambda^3)_{i+1}}, \quad (e_4)_i = \frac{\lambda_i}{2\lambda_{i+1}} - \frac{(EI\lambda^3)_i}{2(EI\lambda^3)_{i+1}}$$

The matrices $S_i(L)$ and M_i in Equation (26) are:

$$S_i(L) = \begin{bmatrix} 0 & 0 & 0 & 0 & 0 & 0 & 0 & 0 & 0 \\ 0 & 0 & 0 & 0 & 0 & 0 & 0 & 0 & 0 \\ -\lambda \sin \lambda L \lambda \cos \lambda L \lambda \sinh \lambda L \lambda \cosh \lambda L & 0 & 0 & 0 & 0 \\ 0 & 0 & 0 & 0 & -\lambda \sin \lambda L \lambda \cos \lambda L \lambda \sinh \lambda L \lambda \cosh \lambda L \end{bmatrix}$$

$$M_i = \begin{bmatrix} m_i & & & \\ & m_i & & \\ & & J_{d,i} & \\ & & & J_{d,i} \end{bmatrix}$$

The matrices $Q_1(0)$ and $Q_n(L_n)$ in Equation (31b) and (31b) are as follows:

$$Q_1(0) = \begin{bmatrix} 1 & 0 & 1 & 0 & 0 & 0 & 0 & 0 \\ 0 & 0 & 0 & 0 & 1 & 0 & 1 & 0 \\ 0 & 0 & 0 & 0 & -E_1 I_1 \lambda^2 & 0 & E_1 I_1 \lambda^2 & 0 \\ E_1 I_1 \lambda^2 & 0 & -E_1 I_1 \lambda^2 & 0 & 0 & 0 & 0 & 0 \end{bmatrix}, \quad (\lambda = \lambda_1 = \tilde{\omega}^{1/2} (\rho_1 A_1 / E_1 I_1)^{1/4}),$$

$$Q_n(L_n) = \begin{bmatrix} \cos \lambda L_n & \sin \lambda L_n & \cosh \lambda L_n & \sinh \lambda L_n & 0 & 0 & 0 & 0 \\ 0 & 0 & 0 & 0 & \cos \lambda L_n & \sin \lambda L_n & \cosh \lambda L_n & \sinh \lambda L_n \\ 0 & 0 & 0 & 0 & -\lambda^2 \cos \lambda L_n & -\lambda^2 \sin \lambda L_n & \lambda^2 \cosh \lambda L_n & \lambda^2 \sinh \lambda L_n \\ \lambda^2 \cos \lambda L_n & \lambda^2 \sin \lambda L_n & -\lambda^2 \cosh \lambda L_n & -\lambda^2 \sinh \lambda L_n & 0 & 0 & 0 & 0 \end{bmatrix}$$

$$\lambda = \lambda_n = \tilde{\omega}^{1/2} (\rho_n A_n / E_n I_n)^{1/4}, \quad L_n \text{ is the length of the } n\text{th shaft segment.}$$

Figure A1 shows a rotating disk i , with a spin speed Ω about its longitudinal axis (a) and a whirling speed $\tilde{\omega}$ about the centreline of the bearings (x_i -axis) or (x_{i+1} -axis). Its axial coordinate is $x = x_i = L_i$ in the fixed coordinate system $x_i y_i z_i$ corresponding to the axial coordinate $x = x_{i+1} = 0$ in the fixed coordinate system $x_{i+1} y_{i+1} z_{i+1}$. abc denotes the cross-sectional coordinate system, defined by the rotational angles $\tilde{\omega}t$, $\bar{\theta}_{y,i}(L_i)$ and $\bar{\theta}_{z,i}(L_i)$ about the x_i -, y_i - and z_i -axis, respectively.

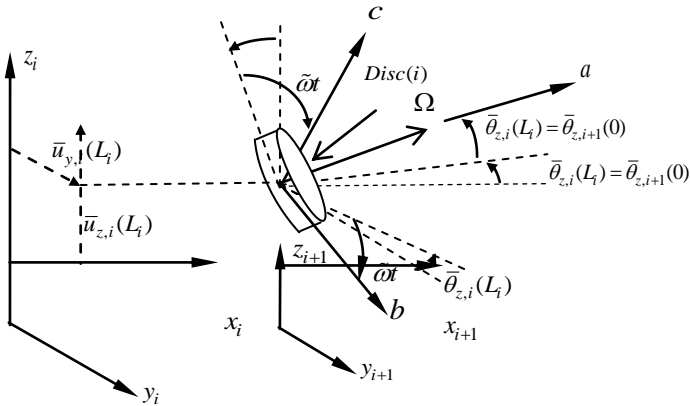


Figure A1: The simultaneous movements of whirling and spinning of a disk.

Figures A2 and A3 show the lowest five natural mode shapes for the pinned-pinned shaft carrying three identical rigid disks. The first, second, third, fourth and fifth natural mode shapes are represented by the curves with solid circles (\bullet), crosses ($+$), triangles (\blacktriangle), squares (\blacksquare), and stars (\star), respectively, as shown in the legend.

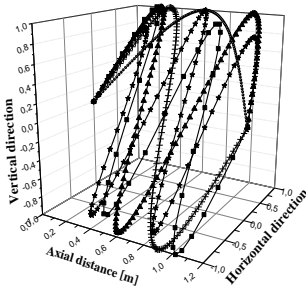


Figure A2: The lowest five natural mode shapes obtained from presented method.

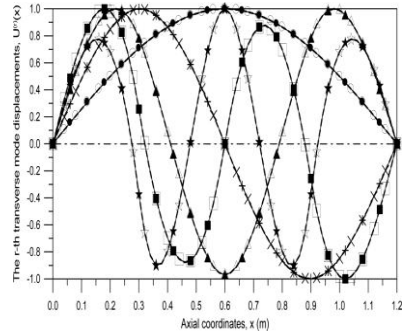


Figure A3: The lowest five natural mode shapes imported from [7].

References

- [1] W. M. Rankine, "On the centrifugal force of rotating shafts," *The Engineer*, vol. 27, pp 249-249, 1869.
- [2] Dunkerley, "On the whirling and vibration of shafts," *Philosophical Transactions on Royal Society of London A*. 185, pp 279-360, 1894.
- [3] F. C. Nelson, "A Brief History of Early Rotor Dynamics," *Sound and Vibration*, vol. 37, no. 6, pp 8-11, 2003.
- [4] R. B. Green, "Gyroscopic effects on the critical speeds of flexible rotors," *Transactions of the American Society of Mechanical Engineers, Journal of Applied Mechanics*, vol. 15, pp 369-376, 1948.
- [5] R. L. Eshleman and R. A. Eubanks, "On the critical speeds of a continuous shaft-disk system," *ASME Journal of Engineering for Industry*, vol. 89, pp 645-652, 1967.
- [6] O. S. Jun and J. O. Kim, "Free bending vibration of a multi-step rotor," *Journal of Sound and Vibration*, vol. 224, no. 4, pp 625-642, 1999.
- [7] Jong-Shyong Wu, F. T. Lin and H. J. Shaw, "Analytical solution for whirling speeds and mode shapes of a distributed-mass shaft with arbitrary rigid disks," *ASME Journal of Applied Mechanics*, vol. 81, no. 3, 034503, 2014.

- [8] R. Surovec, J. Sarlosi and J. Bocko, "Lateral rotor vibration analysis model," *American Journal of Mechanical Engineering*, vol. 2, no. 7, pp 282-285, 2014.
- [9] J. P. Spagnol and H. Wu, "Rotor vibration under the coupled effect of mass unbalance and asymmetric bearings," *Advances of Computational Mechanics in Australia, Applied Mechanics and Materials*, vol. 846: pp199-204, 2016.
- [10] M. Moradi Tiaki, M. Zamanian and S.A.A. Hosseini, "Nonlinear forced vibrations analysis of overhung rotors with unbalanced disk," *Archive of Applied Mechanics*, vol. 86, no. 5, 2016.
- [11] J. Lund and F. Orcutt, "Calculations and experiments on the unbalance response of a flexible rotor," *Journal of Engineering for Industry*, vol.89, pp 785-796 (1967).
- [12] B. Murphy and J. Vance, "An improved method for calculating critical speeds and rotor dynamic stability of turbo machinery," *Journal of Engineering for Power*, vol. 105, pp 591-595, 1983.
- [13] J. Kolenda, "Forced vibrations of shaft line taking in to account the flexural stiffness asymmetry and foundation flexibility," *Journal of Theoretical and Applied Mechanics*, vol. 16, no. 4, pp 517-535, 1978. (In Polish).
- [14] J. Kolenda, "A more precise description of shaft line vibrations," *Journal of Theoretical and Applied Mechanic*, vol. 17, no. 2, pp105-126(1979). (in Polish).
- [15] Ch. Kandouci and Y. Adjal, " Forced axial and torsional vibrations using transfer matrix method related to solution coefficients," *Journal of Marine Science and Application*, vol. 13, no. 2, pp 200-205, 2014.
- [16] P. Natanson, *Short Course in Higher Mathematics, Publ. Lan.(St. Petersburg)*, 399-401 (1999). (In Russian).